Vol. 41 — N° 3 09 17 p. 381 – 396

GEOSTANDARDS and GEOANALYTICAL RESEARCH

Instrumentation Development for *In Situ* $^{40}Ar/^{39}Ar$ Planetary Geochronology

Leah E. **Morgan** (1, 2)*, Madicken **Munk** (3), Brett **Davidheiser-Kroll** (2, 4), Nicholas H. **Warner** (5), Sanjeev **Gupta** (6), Rachel **Slaybaugh** (3), Patrick **Harkness** (7) and Darren F. **Mark** (2)

(1) U.S. Geological Survey, Denver Federal Center, MS 963, Denver, CO, 80225, USA
(2) Scottish Universities Environmental Research Centre, Rankine Avenue, East Kilbride, G75 0QF, UK
(3) Department of Nuclear Engineering, University of California at Berkeley, 3115B Etcheverry Hall, Berkeley, CA, 94720, USA
(4) Department of Geological Sciences, CU Boulder, Boulder, CO, USA
(5) Department of Geological Sciences, SUNY Geneseo, Geneseo, NY, 14454, USA
(6) Department of Earth Science and Engineering, Imperial College London, South Kensington Campus, London, SW7 2AZ, UK
(7) School of Engineering, University of Glasgow, James Watt South Building, Glasgow, G12 8QQ, UK
* Corresponding author. e-mail: lemorgan@usgs.gov

The chronology of the Solar System, particularly the timing of formation of extra-terrestrial bodies and their features, is an outstanding problem in planetary science. Although various chronological methods for *in situ* geochronology have been proposed (e.g., Rb-Sr, K-Ar), and even applied (K-Ar), the reliability, accuracy, and applicability of the $^{40}Ar/^{39}Ar$ method makes it by far the most desirable chronometer for dating extra-terrestrial bodies. The method however relies on the neutron irradiation of samples, and thus a neutron source. Herein, we discuss the challenges and feasibility of deploying a passive neutron source to planetary surfaces for the *in situ* application of the $^{40}Ar/^{39}Ar$ chronometer. Requirements in generating and shielding neutrons, as well as analysing samples are described, along with an exploration of limitations such as mass, power and cost. Two potential solutions for the *in situ* extra-terrestrial deployment of the $^{40}Ar/^{39}Ar$ method are presented. Although this represents a challenging task, developing the technology to apply the $^{40}Ar/^{39}Ar$ method on planetary surfaces would represent a major advance towards constraining the timescale of solar system formation and evolution.

Keywords: geochronology, Ar-Ar dating, mass spectrometry, instrumentation, neutron source.

Received 30 Nov 16 – Accepted 15 Mar 17

Accurate and precise determination of timescales is critical to understanding the history of planetary and asteroidal bodies and is essential to mission planning and the search for extra-terrestrial life. Extra-terrestrial chronologies have been determined to some extent by isotopic analyses of meteorites from Mars and other bodies. Although the planetary or asteroidal parent body of meteorites can often be determined, the exact geographic provenance location is difficult, if not impossible, to ascertain. Thus, age constraints on specific planetary surfaces have thus far been limited to relative techniques such as crater counting, which is not only reliant on calibrations to lunar cratering models (Ivanov 2001) and the analysis of the limited samples returned from Apollo and Luna missions but is dependent on observations and assumptions of the counted surface's complex geological history (e.g., resurfacing and exhumation). Furthermore, crater counting involves significant human interaction and errors that are often not systematic and are not easily quantified (Robbins *et al.* 2014).

Given the success of recent unmanned missions to Mars (e.g., Spirit, Opportunity, Curiosity), development of an *in situ* absolute dating instrument packages for future robotic missions is a logical next step (Cassata 2014, Farley *et al.* 2014). Although several ongoing programmes of research are developing innovative methods for the *in situ* application of the K–Ar technique (Swindle *et al.* 2003, Talboys *et al.* 2009, Cho *et al.* 2012, Farley *et al.* 2013, Cartwright *et al.* 2014, Cohen *et al.* 2014a, b) and other methods (Anderson *et al.* 2012), the nature of the K–Ar method means that these approaches could deliver ages with questionable geological

doi: 10.1111/ggr.12170

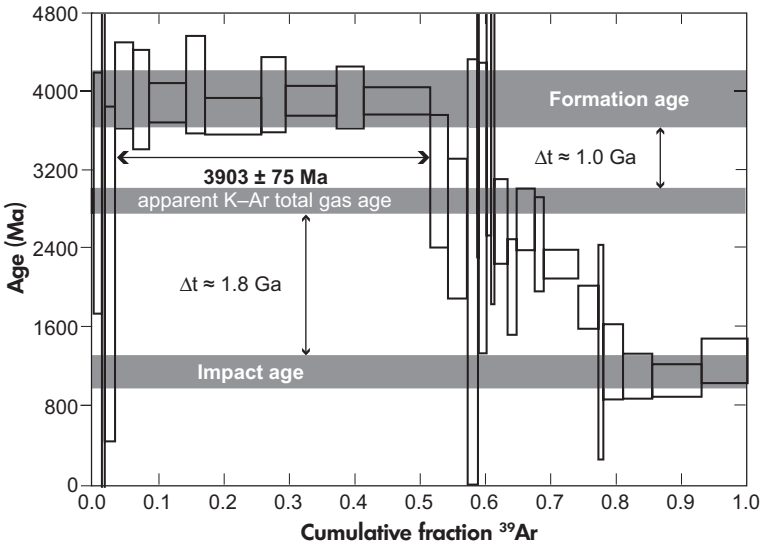

Figure 1. $^{40}Ar/^{39}Ar$ age spectrum for pyroxene from meteorite Allan Hills 84001, modified from Cassata *et al.* (2010), and provided as an example of the effects of thermal events on apparent ages. Approximate formation, impact and apparent K–Ar (total gas) ages are shown as grey bars. Note the difference between the apparent impact and formation ages, as well as the approximate age that would have been determined by application of the K–Ar method to this sample. This illustrates the potential for the K–Ar method to yield biased ages, with no means of identifying that bias. Many extra-terrestrial samples yield similarly complex age spectra.

meaning due to the likelihood of recorded complex thermal histories (Figure 1). This has in particular proved true for lunar samples from the Apollo missions (e.g., Turner 1970a, b, McDougall and Harrison 1999, Boehnke and Harrison 2016) and the unrecognised presence of excess ^{40}Ar.

These potential issues can be circumvented by the application of the $^{40}Ar/^{39}Ar$ variant of K–Ar geochronology (Merrihue and Turner 1966, Li *et al.* 2011, Cassata 2014). The $^{40}Ar/^{39}Ar$ technique allows for the identification of and correction for variable trapped components (e.g., excess ^{40}Ar), and for the resolution of complex thermal and diffusive histories. However, the method relies on the fast neutron-induced $^{39}K(n,p)^{39}Ar$ reaction (transmutation of ^{39}K to ^{39}Ar) so that ^{39}Ar can be measured as a proxy for the parent element K, which typically occurs in a ^{235}U fission reactor. Although the development of a ^{235}U fission reactor for spaceflight has previously been explored via the cancelled Prometheus project (Taylor 2005), the feasible option of exploiting passive neutron sources is explored herein. Within this contribution, we explore the many parameters involved in deploying an instrument package for *in situ* $^{40}Ar/^{39}Ar$ geochronological analyses on extra-terrestrial surfaces.

$^{40}Ar/^{39}Ar$ geochronology

The K–Ar and $^{40}Ar/^{39}Ar$ methods rely on the radioactive decay of ^{40}K to ^{40}Ar and are most often applied to high-temperature igneous and metamorphic mineral phases and rocks. They are founded in the concept that ^{40}Ar atoms produced within a system are only retained when temperatures are sufficiently low to prevent diffusive loss. Typical K–Ar analyses are hampered analytically by the necessity of measuring ^{40}K and ^{40}Ar on separate aliquots, in addition to a mass measurement on each aliquot; many of these analytical issues have been potentially ameliorated with a pioneering technique designed for spaceflight by Farley *et al.* (2013). However, the $^{40}Ar/^{39}Ar$ method has a number of analytical and practical benefits over the K–Ar method. Most critically, the measurement of ^{39}Ar as a proxy for the parent isotope ^{40}K allows for incremental heating of samples and thus interrogation of thermal histories, which is required given the impact features of the planets, moons and asteroidal bodies throughout the solar system. Incremental step-heating data, where a sample has been heated to consecutively higher temperatures over the course of an analysis sequence, can be inspected on an age spectrum plot (Figure 1), where the fraction of total ^{39}Ar released is shown against the age calculated for each step, and isochron diagrams, which can indicate the ratio of trapped argon isotopes at the time of closure. Thus, portions of the age spectrum can be interpreted to represent (and determine a reliable age for) various events in the geological history of the sample, and/or indicate the presence of various complications that can occur in samples, such as excess argon and recoil effects.

One requirement of the $^{40}Ar/^{39}Ar$ method is the creation (transmutation) of sufficient quantities of ^{39}Ar from ^{39}K so that precisely measurable $^{40}Ar/^{39}Ar$ ratios are obtained. High-precision measurements require $^{40}Ar/^{39}Ar$ ratios relatively close to 1, although ratios of 10–100 are routinely measured in terrestrially sourced samples to limit irradiation time and costs. Older rocks, such as those found on extra-terrestrial surfaces, contain more ^{40}Ar ingrown from ^{40}K and thus require larger quantities of ^{39}Ar to be created during irradiation. It is not uncommon during the analysis of meteorites for scientists to be measuring $^{40}Ar/^{39}Ar$ ratios of 300 or even higher (e.g., Bogard and Garrison 2003). In an *in situ* extra-terrestrial situation with a neutron flux limited by design constraints, achieving sufficient neutron fluence to create measurable $^{40}Ar/^{39}Ar$ values in reasonable time-frames becomes a difficult task. The parameters requiring consideration are discussed herein.

Sample availability and selection

The potential utility of inclusion of the system described herein to a future spaceflight mission is largely dependent on the destination of that mission. The K–Ar and $^{40}Ar/^{39}Ar$ chronometers are, by far, most applicable to igneous and metamorphic rocks, as it records the cooling age and/or thermal history of a sample. The appropriate geological interpretation of a recent application (Farley *et al.* 2014) of the K–Ar method to fine sediments on Mars remains elusive, as the age represents the potassium-weighted mean age of a large number of grains and cannot be interpreted as a sedimentation age. The $^{40}Ar/^{39}Ar$ method is thus most powerfully applied in the solar system to volcanic and/or impacted rocks; this could include those from solid planets (e.g., Mars), moons, or smaller asteroidal bodies.

Calibrating Martian crater-counting chronologies

Among the most powerful potential applications of the methods presented here would involve a mission to one of the large igneous provinces on Mars, with the purpose of dating samples across these regions to calibrate crater-counting methods. Crater counting is currently calibrated using the assumption of equivalent impact histories for Mars and the moon (Ivanov 2001), which is itself calibrated by chronological analyses of samples returned from Apollo missions. Direct calibration of the Martian impact history would require careful selection of possible sites for dating. The relatively young, Late Hesperian- to Amazonian-age (< 3.0 Ga) flood lava fields of Tharsis and/or Elysium (Tanaka *et al.* 2014) are ideal targets. Here, diagnostic lava morphologies (e.g., lobate flow features, lava tubes, channels) are obvious, and the areal extent (> 100–1000 km^2) of individual large flood lava flows provides a statistically significant sample of impact craters (e.g., hundreds) to robustly test the dating technique against the impact crater chronology data (Warner *et al.* 2015). Furthermore, Hesperian- to Amazonian-age surfaces have not been exposed to the high impact rate (Hartmann and Neukum 2001, Ivanov 2001) or the high erosion rates (Golombek *et al.* 2006) that characterised the Late Heavy Bombardment period of the Late Noachian epoch. During this time, significant impact gardening and active surface processes (e.g., fluvial and aeolian activity) likely reworked the upper tenth to hundreds of metres of the Martian crust, which would challenge *in situ* identification of an in-place igneous sample (Hartmann *et al.* 2001, Hartmann and Barlow 2006).

Ideally, a mission could, for example, aim to land a rover at a geological contact of Early Amazonian lava plains and the older Hesperian-age ridged plains. Such a location is available at several locations in the northern lowlands proximal to the Elysium volcanic province. The Hesperian-age ridged plains here (Tanaka *et al.* 2014) have been proposed to also represent flood lavas, where the thin, individual flow margins have been blended through 3+ billion years of metre-thick regolith development. In places where the regolith is only metres thick, fresh, rocky ejecta impact craters may provide windows into the near-surface primary volcanic stratigraphy. It may also be possible to capture all three geological epochs within a landing region that could be reasonably traversed by a rover along the planetary dichotomy in southern Elysium Planitia. The ultimate goal of such a mission would be to remove potential biases involved in the derivation of age on Mars using crater counts. This would significantly improve our ability to constrain the chronology of landforms and terrains across the entire surface, including those areas being explored for signs of life by Curiosity, the Mars 2020 mission and the ExoMars mission.

Other potential uses of technology

A critical goal of the forthcoming Mars 2020 mission will be to collect a cache of samples for their eventual return to Earth. In the event that this return mission is not possible, a lander mission to the site of the sample cache could be deployed to analyse samples from the cache on Mars. Similarly, the technology described herein could also be deployed on a lander or rover mission to asteroids and other solid planetary bodies whose surfaces are dominated by igneous processes (e.g., the Moon). Further, plans for future sample return missions from Mars will include sample containment facilities and protocols. If samples are to remain within a closed facility, the neutron source technology described herein could be installed to allow for in-house

sample irradiation. In this case, shielding requirements would be significantly higher, but mass restrictions significantly less stringent. Alternative neutron sources for this application are D-D type (Renne *et al.* 2005), D-T type neutron sources.

Sampling and sample handling

Samples for $^{40}Ar/^{39}Ar$ geochronology can be in the form of rock chips as small as *ca.* 100 μm, limited by the increased effects of nuclear recoil on small grain sizes (e.g., Paine *et al.* 2006, Jourdan *et al.* 2007). Samples of this size are most readily collected by drilling, which can take two forms, core drilling and powder drilling, both of which have undergone development for other extra-terrestrial exploration purposes.

Core drilling

Sampling and encapsulation of larger rock fragments in the form of a core can be achieved in a single process if the sample is extracted within the cutting bit and the bit is subsequently sealed (Timoney *et al.* 2015). Coring bits with a centre drill can produce toroidal core samples, and ultrasonic percussive drilling techniques can produce core samples that need not necessarily exhibit rotational symmetry (Bar-Cohen and Sherrit 2003). These options raise the possibility of packing bespoke sample capsules around the neutron source made from material with a small total cross section, thus maximising the neutron activation of ^{39}K in the sample.

Powder drilling

An alternative to core drilling is powder drilling. In this case, grain sizes may be sorted by sieving prior to analysis, but high-amplitude vibration that could be damaging to the instrument package is not necessarily required. Ultrasonic actuation of the sieves and associated chutes can agitate and aid transport of the material in a manner similar to that currently employed on the CheMin instrument. The receiving hopper associated with each sieve may then be shaped and employed as a sample capsule, as with the core drilling methods. Ideal grain sizes, based on terrestrial applications, are 250–500 μm.

Neutron generation

Although terrestrial application of the $^{40}Ar/^{39}Ar$ method typically relies on neutrons produced by a ^{235}U fission reactor, the deployment to planetary surfaces of a reactor at nuclear criticality is unlikely. The approach taken here, similar to that of Li *et al.* (2011), instead involves a transport and exploitation of a passive neutron source. The most viable passive neutron source is ^{252}Cf, with its relatively high neutron flux by mass (*ca.* 2.33×10^9 n s^{-1} for each mg of material) and relatively low specific heat output compared with other passive neutron sources (Table 1). Challenges in deploying this source are (1) it has a relatively short $t_{1/2}$ of 2.645 years and (2) ^{252}Cf is difficult to produce; as of the year 2000, the HFIR at ORNL typically produced *ca.* 250 mg per year (Martin *et al.* 2000). Obtaining sufficient neutron fluence from reasonable quantities of source material over reasonable irradiation durations is a major limitation and is addressed herein.

The required neutron flux for sample irradiation depends largely on the abundance of K and the sample age (amount of radiogenic ^{40}Ar). In terrestrial applications, a $^{40}Ar/^{39}Ar$ ratio of 100 on a 4 Ga sample can be obtained, for example, by a 13.6 day irradiation in the fast neutron flux of 2.47×10^{13} n cm^{-2} s^{-1} in the CLICIT Facility of the Oregon State University TRIGA Reactor (see Figure 2). This yields a total neutron fluence of 2.90×10^{19} n cm^{-2}. In comparison, the entire 40 mg of ^{252}Cf made in some production runs at ORNL would yield *ca.* 1×10^{11} n s^{-1}, resulting in a neutron flux (at 1 cm distance from the source) of just *ca.* 8×10^9 n cm^{-2} s^{-1}, over three orders of magnitude lower than the OSU reactor. However, this is very slightly ameliorated by the neutron energy spectrum for ^{252}Cf, which is somewhat faster than that

Table 1.
Passive neutron sources decaying by spontaneous fission

Source material	Mass required for 10^{11} n s^{-1}	Flux (n s^{-1} mg^{-1})	$t_{1/2}$ (years)	SF branching ratio (%)	Heat output (W/10^{11} n s^{-1})
^{252}Cf	43 mg	2.3×10^9	2.645	3.82	1.43
^{250}Cf	9.5 g	1.1×10^7	13.08	0.08	31
^{248}Cm	2.14 kg	4.7×10^4	3.5×10^5	8.26	1.04
^{246}Cm	9.8 kg	1.0×10^4	4.7×10^3	0.03	90
^{244}Cm	9.8 kg	1.0×10^4	18	1.3×10^{-4}	2.4×10^4
^{253}Es	274 g	3.6×10^5	0.05	8.7×10^{-6}	2.1×10^5
^{254}Fm	0.2 mg	3.4×10^{11}	3.7×10^{-4}	0.06	33

^{252}Cf was selected here as the most desirable neutron source due to its availability, high neutron flux per unit mass and low heat output. Heat output is provided in W produced by the mass required to achieve source strengths of 10^{11} n s^{-1}.

of ^{235}U fission and thus improves the efficiency of the ^{39}K(n,p)^{39}Ar reaction (Figure 3).

It is possible to increase the neutron flux via the use of neutron booster material. These materials undergo neutron-emitting reactions when exposed to a neutron source. For example, the reactions ^{9}Be(n,2n)^{8}Be and ^{9}Be(n,3n)^{7}Be, along with the neutron-induced fission reactions on ^{233}U, ^{235}U, ^{239}Pu, ^{240}Pu and ^{241}Pu, all emit more neutrons than required for the reaction. Below, we explore the use of ^{252}Cf and the potential for neutron flux booster material as a means of increasing the neutron flux to limit the irradiation duration and achieve acceptable ^{40}Ar/^{39}Ar ratios that facilitate reasonably precise age determinations (Figure 2). Further details on neutron generation are available in Munk *et al.* (2015).

Simple ^{252}Cf source geometry

The simplest neutron source geometry considered here includes a point source of ^{252}Cf, surrounded by a space for samples and reflective shielding material (Figure 4a). Monte Carlo Neutron Particle (MCNP) modelling shows that the neutron energy spectrum within the sample chamber (Figure 5) is relatively fast, with a fast peak in the MeV range, reflecting the neutron energy spectrum of fission-born neutrons. The *y*-axis in Figure 5 normalises the flux to units of lethargy, which accounts for the scattering efficiency of the incident material.

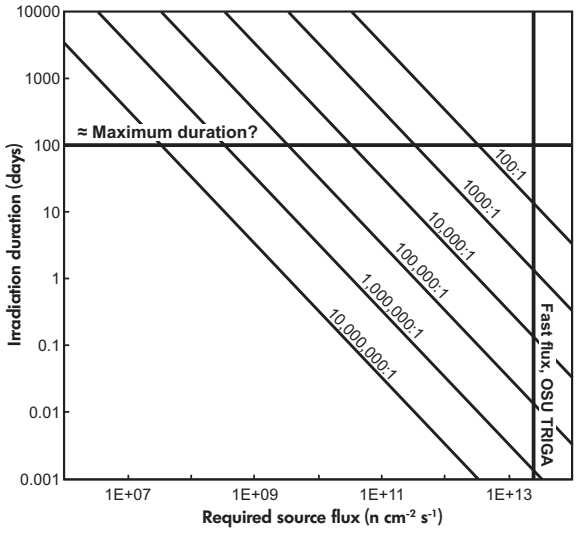

Figure 2. Required source flux and irradiation duration to reach various ^{40}Ar/^{39}Ar ratios for a 4 Ga sample. Diagonal lines represent different ^{40}Ar/^{39}Ar ratios; movement along a line shows the range of source fluxes and irradiation durations required to attain that ratio. The fast neutron flux (2.5 × 10^{13} n cm^{-2} s^{-1}) in the CLICIT facility of the Oregon State University TRIGA reactor is shown for reference, as is a maximum 'reasonable' but arbitrary irradiation duration of 100 days. For example, a ^{40}Ar/^{39}Ar ratio of 10^{5}:1 can be reached with a *ca.* 3.3 × 10^{9} n cm^{-2} s^{-1} neutron flux over *ca.* 100 days. Note that neutron flux at launch will decrease over the lifetime of the mission, given the $t_{1/2}$ of ^{252}Cf of *ca.* 2.6 years.

Complex spherical geometry

Spherical geometries that include concentric spheres with a ^{252}Cf point source at the centre surrounded by a void for samples, booster/multiplier material and shielding were explored (Figure 4b). A spherical design should yield the most efficient boost per unit mass, relative to the complex cylindrical geometries described below. Several booster materials were considered as neutron multiplier materials, including ^{9}Be, ^{233}U, ^{235}U, ^{239}Pu, ^{240}Pu and ^{241}Pu (Figures 6 and 7). We used a spherical geometry as shown in Figure 4b, with 90% enriched ^{235}U and 100% enrichment for other transuranic metal oxides and Premadex® as a reflector material. Modelling indicates that the most efficient multipliers are ^{239}Pu and ^{241}Pu, as shown in Figure 7.

Complex cylindrical geometry

A more complex cylindrical geometry can also be considered, with rotatable or extractable 'pins' composed of neutron multiplicative material (e.g., ^{9}Be, ^{233}U, ^{235}U, ^{239}Pu,

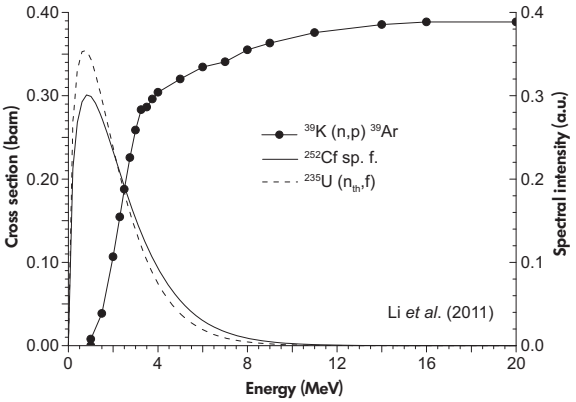

Figure 3. Neutron energy spectra for ^{252}Cf and ^{235}U, using parameters corresponding to their respective Watt fission spectrums, along with the modelled neutron capture cross section for the ^{39}K(n,p)^{39}Ar reaction from ENDF. Note that the ^{252}Cf spectrum is slightly higher energy than the ^{235}U spectrum, and thus more favourable for the ^{39}K(n,p)^{39}Ar reaction. Reproduced from Li *et al.* (2011).

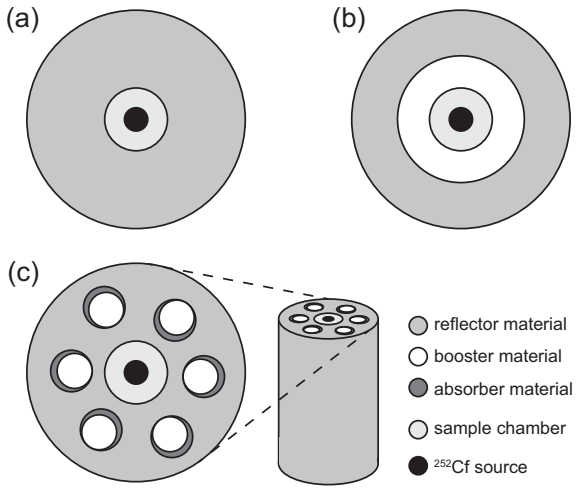

Figure 4. Neutron source geometries explored and modelled herein. (a) Cross section of concentric spherical source, with point source of ^{252}Cf surrounded by spherical sample chamber (void) and reflector material. (b) Cross section of similar concentric spherical source, with the addition of ^{235}U neutron booster or multiplier material. (c) Overhead and side views of cylindrical source, with central ^{252}Cf source surrounded by sample chamber (void) and reflector material. ^{235}U neutron multiplier material is located in rotatable or removable pins to allow for control over source neutron flux.

^{240}Pu, ^{241}Pu) and backed by neutron-absorbing material (Figure 4c). This arrangement allows for a somewhat 'switchable' source, where the flux is enhanced when fissionable material faces the source and depressed when the 'pins' are rotated and absorbent material faces the source. Given sufficiently high multiplicative effects, this could serve to boost the neutron flux so that irradiation could occur in a reasonable time period (see Figure 2 for values) while reducing the total neutron fluence seen by other instruments in the mission. This geometry may also be utilised to maintain a constant neutron flux over the course of a mission, as the decay of ^{252}Cf decreases the flux from the ^{252}Cf source itself.

Neutron shielding

Neutron shielding is important to prevent radiation damage to the rover or lander system and potentially also to prevent irradiation of the extra-terrestrial surface. Neutron shielding requirements are ultimately limited by rover tolerances to an elevated neutron flux. Estimations of acceptable neutron flux tolerances for the current Curiosity rover mission are considered sensitive material by International Traffic in Arms Regulations (ITAR) and thus have not been accessible. However, some indication as to acceptable fluxes can be derived both from experiments included with the Curiosity mission and from the most sensitive components included in that mission. Towards this, the Dynamic Albedo of Neutrons Pulse Neutron Generator (DAN-PNG) experiment, which is designed to search for hydrogen, and thus water, on the surface and subsurface of Mars, emits short (1 μs) but high-energy (14 MeV) pulses of 10^7 neutrons (Mitrofanov *et al.* 2005, 2012, Litvak *et al.* 2008). A further constraint can be estimated based on the CCD (charge coupled device) image sensors on Curiosity from Teledyne DALSA in collaboration with NASA and should be among the most neutron sensitive components on Curiosity. These CCD devices are radiation hardened and are designed to tolerate radiation doses of up to 200–300 Gy (D. Head, personal communication 2014), which equates to *ca.* 4×10^{13} n cm^{-2} (United States Nuclear Regulatory Commission 2014) and provides a starting point for shielding calculations. Actual required shielding will depend on the allowed tolerances for future missions, which may be less stringent than those assumed here, and information is provided here to allow for recalculation based on those limits.

The effects of neutron flux on the system are complex, and several of these must be considered. For example, secondary effects can create radioactive elements due to the neutron irradiation of elements present in the system (e.g., Fe). Further, neutron irradiation of sensitive electronics components can affect the system in multiple ways, including first-order displacement of atoms due to neutron bombardment and single-event digital effects on semiconductor materials. The magnitude of these effects is dependent in part on the energy spectrum of the field, and selection of shielding materials will need to consider this. A future consideration would also incorporate shielding of the high-energy photons yielded by ^{252}Cf fission products. An additional consideration for shielding involves mitigating activation of the shield and rover material by the source neutrons. Further details on neutron shielding are available in Munk *et al.* (2015).

Shielding materials

Neutron shielding materials considered here include high-density polyethylene (HDPE), B_4C, Premadex®, ^{6}Li-enriched Premadex® and Gd. These materials can act either (1) to scatter and decrease neutron energy, for example, HDPE and Premadex®, or (2) to absorb neutrons by nuclear reaction, for example, B_4C, Gd, Cd and Li. The relative efficiencies of these materials are provided in Figure 8 and include neutrons with an energy spectrum from a ^{252}Cf fission source. Shield efficiency is considered

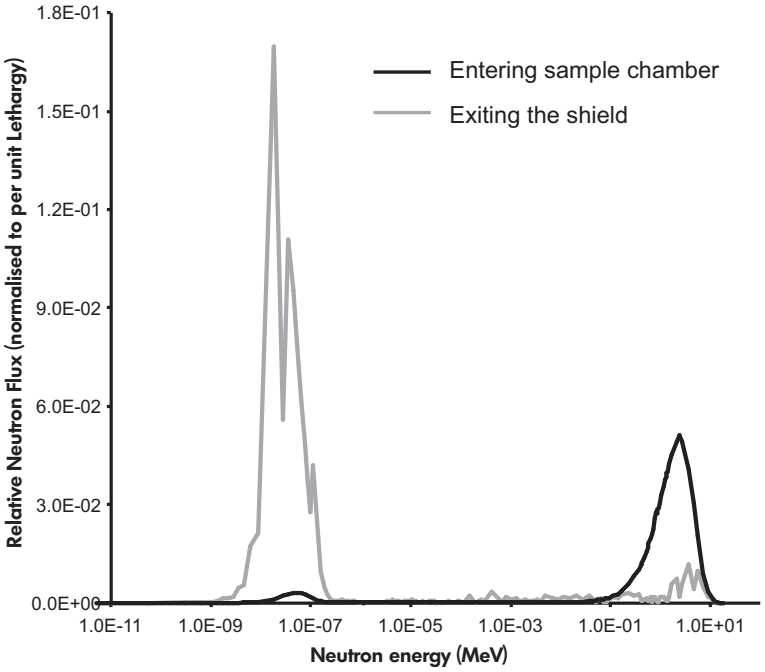

Figure 5. Results from MCNP modelling of neutron flux in simple spherical source (e.g., Figure 4a) with a 30 cm thick HDPE shield. Modelled neutron energy spectrum in sample chamber (black) and those neutrons that escape from the shield (grey). Energies of many neutrons exiting the shield are lower due to scattering in the low-Z shield material. The neutron flux in the *y*-axis is normalised to lethargy, which accounts for the scattering efficiency of the incident material.

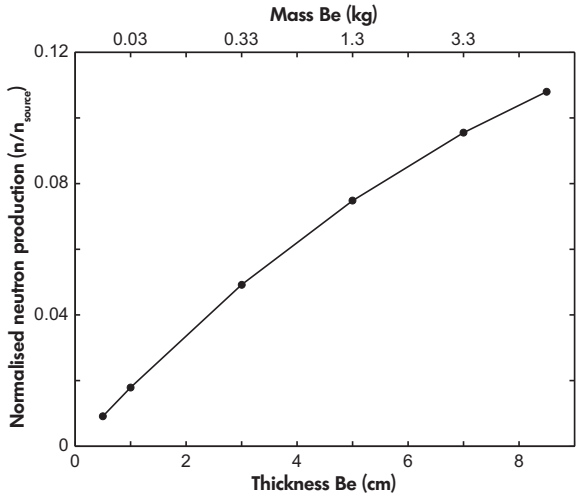

Figure 6. Results from MCNP modelling of spherical source geometry as in Figure 4b. Efficiency of ^{9}Be multiplier with a range of thicknesses and masses, representing the additional neutrons created by the multiplier. Model completed using Premadex® as reflector material; reflector thickness did not appreciably affect results.

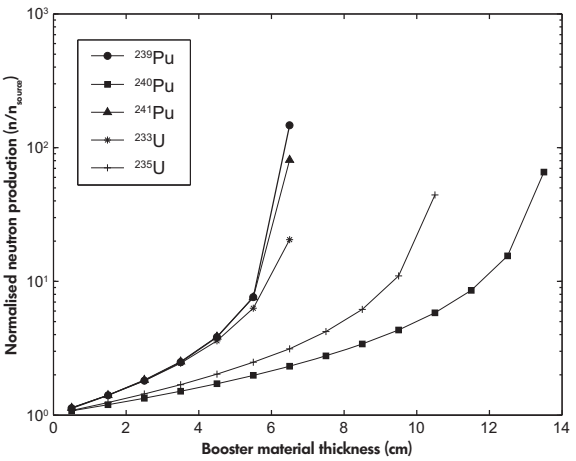

Figure 7. Results from MCNP modelling of spherical source geometry as in Figure 4b. Multiplication efficiencies of 90% enriched $^{235}UO_2$ and 100% enriched other transuranic isotopes are shown against thickness and mass of booster material. Models completed using Premadex® as reflector material; reflector thickness did not appreciably affect results. Similar results are found with variable sample void radii.

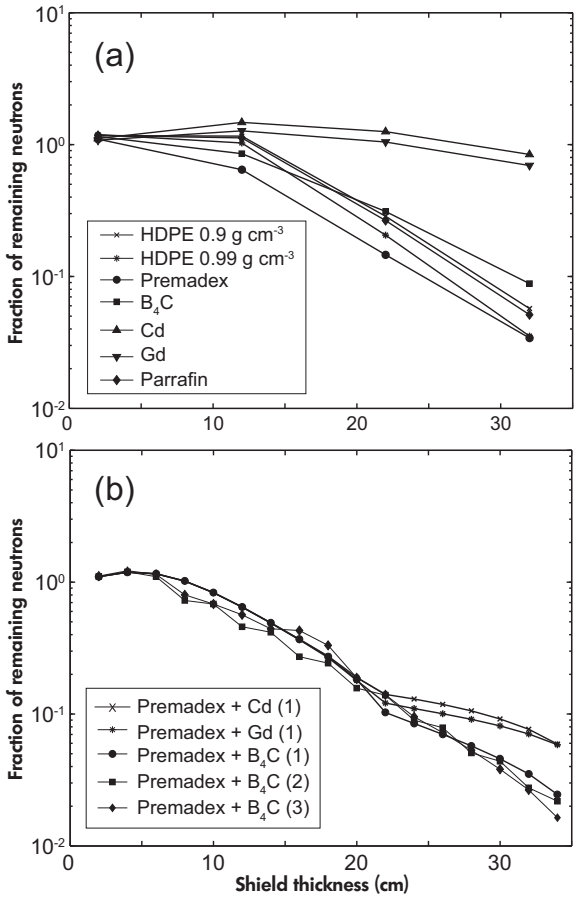

Figure 8. Results from MCNP modelling showing the efficiencies (provided as a fraction of remaining neutrons) of various shield materials, based on a simple concentric spherical geometry (Figure 4a). Note that efficiencies are based on collisions within the material and do not account for geometric effects. Neutrons of all energies are included in calculations. (a) Shield efficiencies for high-density polyethylene (HDPE), Premadex®, B_4C, Cd, Gd and paraffin. See Figure 5 for neutron energy spectrum for HDPE shield. (b) Shield efficiencies for composite shields of Premadex® combined with a variety of materials. (1) 20 cm of Premadex® surrounded by 14 cm of the other material. (2) B_4C alternates with Premadex® every 2 cm in the shield. (3) Premadex® with two layers of B_4C, of 8 cm and 6 cm thickness.

here as a 'fraction of remaining neutrons' and importantly does not consider geometric effects, which further decrease the effective flux by the square of the distance away from the neutron source and are considered separately.

Shielding a simple ^{252}Cf source

To better understand the energy spectrum of neutrons exiting shield material, the simple spherical source (Figure 4a) is modelled using 30 cm of HDPE as a shield. The energy spectrum of neutrons exiting the shield is provided in Figure 5. Note that many neutrons exiting the shield are thermalised to 10^{-7}–10^{-8} MeV, which represent neutrons that have been downscattered, or moderated, in the shield from fast to thermal energies. Figure 8 shows the fraction of remaining neutrons in the system across the shield, for (a) various materials and (b) several composite shields. The most efficient shield would likely include a moderator to thermalise neutrons, with foils of a strong neutron absorber (e.g., Cd or Gd) with a high thermal neutron capture cross section to remove the thermalised neutrons.

Geometric effects aid neutron flux mitigation by the inverse square rule; the reduction in flux due to distance from source (and not including attenuation due to shielding) follows the inverse square of distance. The relative effect is such that a source with a 10^{11} n cm^{-2} s^{-1} flux at the sample chamber would decrease to 4×10^7 n cm^{-2} s^{-1} at 50 cm distance from the source. Further, the amount of shielding required can also be decreased due to geometric effects, if one considers shielding only the rover and not the planetary surface and/or atmosphere. For example, a neutron source located at 1 m distance from a region of 1 m^2 of sensitive components would only need to cover *ca.* 6% of the surface area of the source.

Radiation, launch clearance and planetary protection

The inclusion of a neutron source in an instrument suite for planetary exploration creates numerous safety considerations, for humans, other instruments and planetary protection. The ^{252}Cf source would need to be added late in the manufacturing process, not only for human safety concerns but also due to its relatively short $t_{1/2}$ and thus significant decrease in neutron flux with time. Appropriate shielding would be required during installation and launch to maintain acceptable human safety conditions.

The possibility of a catastrophic launch must also be considered. The neutron source in particular needs to be encased so that it retains radioactive material during a launch failure situation. Further, the inclusion of any fissionable booster material in the source must remain below criticality levels in any accident scenario, including the case of potentially high pressures experienced during a crash landing situation. The potential for long-term radioactive contamination is low due to the relatively short $t_{1/2}$ of ^{252}Cf, but daughter products may also be problematic. In particular, spontaneous fission (SF) produces a range of daughter isotopes and alpha decay produces ^{248}Cm

($t_{1/2}$ = 3.5 × 10^5 years), which subsequently decays by both SF and alpha decay to ^{244}Pu ($t_{1/2}$ = 80 Ma). Ultimately, launch requirements must meet local environmental standards [e.g., the National Environmental Policy Act (NEPA)].

Planetary protection is critical to the feasibility of the mission. Although traditional planetary protection has been concerned with interplanetary biological and chemical contamination, this instrumentation introduces the possibility of exposing planetary or lunar surfaces to significant neutron fluxes, which could affect existing biology and chemistry on the surface. Issues associated with this must have been addressed to some extent by the DAN instrument included on the Curiosity rover, but flux and fluence levels involved here are significantly higher and must be considered. Although shielding could theoretically reduce these levels, the increased mass of shielding required to protect the entire surface and/or atmosphere (rather than only the rover or lander) is considerable. This is discussed in detail in the feasibility analysis below.

Gas extraction and analysis

^{40}Ar/^{39}Ar geochronology requires heating to release argon from the material to be dated. The resultant gas is then cleaned to trap reactive gases and isolate noble gases for mass spectrometric analysis. Below, we describe parameters involved in application of these requirements to spaceflight, relying when possible on flight-ready instruments included as part of recent or existing missions.

Sample heating and gas extraction

Samples must be heated to release Ar gas for analysis. In terrestrial applications, this is accomplished using a furnace or laser, with desired temperatures of up to 1200 °C, depending on the melting temperature and melt viscosity of the sample. These temperatures would prove difficult to reach given recent power capabilities of rover furnaces. For example, the oven in the Sample Analysis at Mars (SAM) instrument suite on the Curiosity rover can heat samples to 950 °C, and up to 1100 °C using an auxiliary heater (Mahaffy *et al.* 2012). This can be ameliorated by analysing smaller grain sizes but also by mixing samples with a lithium borate flux (similar to those used in preparing glass beads for XRF analysis) prior to heating; experiments using this type of flux have been shown to completely degas basaltic samples at *ca.* 965 °C (Farley *et al.* 2013). However, the use of a flux may affect incremental heating release patterns; this issue should be a major component of future testing, to ensure that argon release patterns are not appreciably affected by use of the flux.

Gas purification

In terrestrial applications, noble gases (of which argon is typically the largest component) are purified using solid-state getter material that traps reactive gases. Such systems have been included successfully in the SAM instrument (Mahaffy *et al.* 2012) and could be used again for a future geochronological mission.

Mass spectrometry

Isotopic ratio measurements for ^{40}Ar/^{39}Ar geochronology are typically made by magnetic sector mass spectrometers. However, magnet masses are prohibitively high for spaceflight and thus recent missions have relied on lower precision quadrupole mass spectrometers, which use energy filters to separate isotopes for detection (Mahaffy *et al.* 2012).

Abundance sensitivity

Among the most important parameters for our purpose is abundance sensitivity, defined as 'the ratio of the maximum ion current recorded at a mass m to the ion current arising from the same species recorded at an adjacent mass ($m \pm 1$)' (McNaught and Wilkinson 1997, p. 1554). Abundance sensitivity is a function of the peak shape and mass resolution of the instrument, and is typically inferior in quadrupole instruments. This is particularly important here, as improved abundance sensitivity allows for the measurement of larger isotopic ratios (e.g., ^{40}Ar/^{39}Ar), and in turn allows for a lower strength neutron source.

Improving the abundance sensitivity of the quadrupole instrument would significantly affect the required neutron source parameters, as it allows for the measurement of larger isotopic ratios. For reference, the Thermo Scientific ARGUS VI magnetic sector mass spectrometer has an abundance sensitivity for the mass 40 tail onto mass 39 of $\leq 5 \times 10^6$. This indicates that for every 5 million ions of ^{40}Ar, one is measured erroneously as ^{39}Ar.

The heritage quadrupole included in SAM has an abundance sensitivity of *ca.* 10^5. However, commercially available gas-source quadrupole instruments, including the Hiden HAL series 1000 triple-filter quadrupole instrument used in terrestrial ^{40}Ar/^{39}Ar work (Schneider *et al.* 2009) and the Extrel MAX series, evidently reach abundance sensitivities of 10^7, representing a potentially significant improvement. Further, plasma-source quadrupole instruments have been modified to yield abundance sensitivities in the mass 40 range of 10^9–10^{10}, using auxiliary quadrupolar excitation to improve peak shape and tailing

characteristics (Konenkov *et al.* 2001). This technology is apparently available commercially through AB SCIEX but does not yet seem to include gas-source instruments, and is not spaceflight ready.

Although significant technological development is required to yield flight-ready quadrupole instruments with high-abundance sensitivities, it appears that reaching abundance sensitivity values of 10^7, and even 10^{10}, is feasible. These values are used herein to consider the ultimate feasibility of the project and could represent a 100- to 10000-fold improvement in abundance sensitivity.

Isobaric interferences

The quadrupole mass spectrometer that is part of SAM has been shown to have significant isobaric interferences from hydrocarbons in the mass range of interest (m/z = 40–36) (Malespin *et al.* 2014). Indeed, the K–Ar age published by Farley *et al.* (2014) relies on the correction of ^{40}Ar signals using separately measured mass 40 to mass 39 hydrocarbon ratios. Isobaric interference could thus create a significant problem on mass 39, which requires the measurement of relatively small ^{39}Ar signals. This issue could be resolved via measurements of hydrocarbon ratios including, for example, mass 41, which could theoretically be used to correct for all argon isotopic measurements in a method similar to that of Farley *et al.* (2014). These corrections would be made using measurements of ratios of mass 41 hydrocarbon to hydrocarbons at all other masses of interest; these ratios would then be used to correct the measured argon isotopic values. It should be noted that the application of this method to mass 39 may be more difficult than the high-mass 39 hydrocarbon signal (relative to mass 40 hydrocarbon), and the low ^{39}Ar signal (relative to ^{40}Ar).

Interfering nuclear reactions

As with terrestrial applications of the ^{40}Ar/^{39}Ar method, nuclear reactions will occur on several common rock-forming elements that can affect calculated ages. Important reactions include ^{40}Ca(n,nα)^{36}Ar, ^{40}Ca(n,α)^{37}Ar, ^{42}Ca(n,α)^{39}Ar and ^{40}K(n,p)^{40}Ar. As with terrestrial applications, these interfering reactions can be corrected for by measurements of high-purity potassium-rich glass and CaF_2 samples, which separate the effects on K and Ca. These measurements could be made during testing prior to launch, but it may be desirable that K-glass and CaF_2 reference materials be included in the launched instrument to monitor potential changes in the neutron energy spectrum over time.

Sensitivity and ion detection

The absolute sensitivity of the instrument is of secondary importance, as increasing sample size can ameliorate issues with low sensitivity. Heritage technology available from SAM (adapted from previous missions) includes an ion source and two continuous dynode secondary electron multipliers. This technology could be readily used for this purpose, but instrument stability may be improved by considering the use of high-gain Faraday amplifiers in addition to the electron multipliers. Although 10^{12} Ω resistors have been in use for some time, recent developments have yielded reliable 10^{13} Ω resistors (Koornneef *et al.* 2014). Further, a UK company (TIA Systems) has partnered with SUERC to develop 10^{14} Ω resistors. These developments may allow for the replacement of multiplier systems with more stable Faraday detector technology with similar sensitivity characteristics.

Detector linearity

The potential for nonlinearity of detectors (either Faraday cup or electron multipliers) must be considered when measuring large isotopic ratios. Faraday detectors have fewer issues with respect to linearity and may be more appropriate for this reason. Prelaunch testing of any detector (s) would of course be necessary to indicate the care required during analyses. Linearity calibrations could be made using a reference material glass (or multiple glasses) with previously determined high ^{40}Ar/^{39}Ar ratio(s).

Analytical methods

Samples are typically run in series with measurements of background and isotopic fractionation in the system. Background values can be determined by following sample analysis procedures without heating a sample. Isotopic fractionation, or discrimination, can be determined by measuring a gas with a known ratio, typically the atmospheric ^{40}Ar/^{36}Ar. This could be accomplished extra-terrestrially by including small fragments of silicate glass that has been heated under the atmosphere and shown to have a specific (likely near-atmospheric) ratio. These glass fragments would be produced on Earth and included in the launch package so that they can be occasionally heated to determine the mass discrimination of the system during analysis.

The ^{40}Ar/^{39}Ar method is a relative method, which requires the analysis of a co-irradiated reference material (RM) used as a neutron flux monitor. Analyses of reference materials would have to be made for each sample that has a unique irradiation history. Given the analytical precisions required for this method, analyses of RMs could be limited to

just a few per sample. Given that each sample step-heating run requires a number of analyses (probably 5–10), while analyses of RMs can be run as total fusions, the latter thus would not significantly increase measurement time.

Feasibility analysis

Many complex parameters, as discussed above, are involved in the deployment of an extra-terrestrial *in situ* $^{40}Ar/^{39}Ar$ geochronology device using a passive neutron source and quadrupole mass spectrometer. These parameters are discussed in combination here to identify potential opportunities for the future application of this method. Issues considered include mass, power, data quality, analysis time and cost.

Requirements

System requirements are twofold:

1 To create sufficient ^{39}Ar during irradiation in a reasonable length of time for measurement of precise (e.g., 5%) $^{40}Ar/^{39}Ar$ ratios on rocks as old as 4.6 Ga.
2 To release argon from rock samples by heating and measure argon isotopes (masses 40, 39, 38, 37 and 36) on released gas.

Mass limitations

Mass is an important consideration for spaceflight applications due to high launch costs. For planetary applications of this technology, mass then is among the most important considerations. For use in an Earth-side containment facility, however, mass is significantly less constrained.

Among the benefits of relying on ^{252}Cf as a passive neutron source is the small mass (43 mg) required to obtain a source strength of 10^{11} n s^{-1} (Table 1). However, as discussed below, ^{252}Cf is an extremely expensive material, and 43 mg is approximately the amount produced annually in the United States. We thus consider the use of neutron multiplier ^{235}U, which would add significant mass to instrument package (Figure 7) but may allow for less ^{252}Cf to be used, and/or balance out the effects of ^{252}Cf decay over the life of the mission. This may also allow for a 'switchable' source, which would act to reduce total fluence seen by instruments (and humans prior to launch). The use of a multiplier could theoretically allow for a rover system to temporarily leave the source and shielding behind for the period of irradiation, and return to collect them when it has switched to lower flux levels. This approach could significantly limit the required shielding, as discussed below. However, the addition of a ^{235}U multiplier would add considerable mass, requiring *ca.* 10 kg for a multiplication factor of 2, and nearly 50 kg for a factor of 10. Neutron multipliers could more readily be used as part of a neutron source to be built in a containment facility for returned samples.

Another major component of the mass budget is neutron shielding. In particular, shielding must protect other mission instruments, potentially the planetary surface, and humans during preparation and launch. Shield materials act to absorb and/or moderate neutrons, and in the process decrease the total neutron energy (Figure 5). Potential shield materials and composite shields have been assessed for their shielding efficiency with respect to mass and thickness (Figure 8). Neutron moderators investigated here are Premadex, HDPE, Paraffin and B4C. Neutron absorbers are Premadex (due to its ^{6}Li content), B_4C, Cd and Gd. Note that neutron absorbers more effectively absorb thermal neutrons and thus can act to increase the relative fast: thermal neutron ratio even while decreasing the total neutron flux. Composite shields containing materials with both moderating and absorbing properties are likely to be the most effective, as moderating material acts to decrease the energy of fast neutrons; the resultant thermal (or epithermal) neutrons can then be more effectively stopped by absorbing material.

Importantly, results in Figure 8 do not incorporate the geometric effect, which relies purely on distance from the source and does not require shielding material. This effect is quite considerable (e.g., decrease in flux of 10^4 over 1 m of space). Implementing this effect would require carefully locating the source within the instrument package so that the most sensitive instruments are at the greatest distance from the source. Although some shield material will no doubt be useful in moderating neutron energies, employing this geometric effect will be integral to the mass-efficient application of this technology to planetary surfaces. The mass of shielding may also be reduced geometrically, depending on the planetary protection concerns, if irradiation of the planetary surface and atmosphere is acceptable.

Although much of the technology required for $^{40}Ar/^{39}Ar$ analyses can be realised using equipment from previous missions, there exists room for improvement in mass spectrometry. The quadrupole instruments described in the above section on mass spectrometry would allow for at least 100-fold improvement in abundance sensitivity, which would decrease the required ^{39}Ar production, thus the required neutron fluence. This affects mass by limiting the required source strength and thus multiplier material and shielding required to produce measurable $^{40}Ar/^{39}Ar$ values over reasonable irradiation durations. However, these improved

quadrupole instruments also have higher mass. For example, the Hiden HAL series 1000 triple-filter instrument described above has a quadrupole filter of *ca.* 0.5 kg and RF generator of *ca.* 15 kg, while the Extrel MAX series instrument weighs *ca.* 40 kg in total. It should be noted that these Earth-based instruments have not likely been constructed with the intention of limiting the mass of the instrument. In contrast, the entire SAM instrument suite on Curiosity, including a quadrupole, gas chromatograph, tuneable laser spectrometer and sample handling capabilities, also weighs 40 kg. However, it may be more mass- and cost-efficient to utilise these improved spectrometers, or lower mass derivations of them, rather than rely on increased ^{252}Cf and shielding, to achieve the same measurement precision.

Power limitations

One benefit of using ^{252}Cf is that as a spontaneous fission neutron source, it requires no power. Minimal power may be required if a 'complex cylindrical geometry' with moveable or rotatable pins of multiplier material is utilised. Further power requirements include sample drilling and handling, sample heating during gas extraction and mass spectrometry. The first two of these should not vary considerably from requirements in SAM, as heating samples in contact with a lithium borate flux may act to effectively decrease the melting temperature of the sample to temperatures accessible by the furnace on SAM (Mahaffy *et al.* 2012, Farley *et al.* 2013).

The implementation of a quadrupole mass spectrometer with improved abundance sensitivity would likely require more power than the QMS on SAM due in part to the higher power requirements for generating the RF field. For example, the Hiden HAL series 1000 triple-filter instrument typically draws *ca.* 260 W, with an absolute maximum of *ca.* 650 W. This can be compared with the available power from the MMRTG on Curiosity, which has a maximum of 110 W, although 42 Ah batteries do allow for higher power draws.

The high power draw of typical high-resolution quadrupole instruments presents an issue that would need to be addressed prior to implementation. Alternatively, a solution could involve development of a high-resolution ion trap mass spectrometer such as one from the Ptolemy instrument on the Rosetta mission (Todd *et al.* 2007) for stable isotopes, and one in development at the Jet Propulsion Laboratory and California Institute of Technology (Neidholdt *et al.* 2015).

It should also be considered that heat generated within the neutron source could be used to partially power the mission, in addition to the MMRTG units used on recent missions.

Data quality

The primary motivation for developing this technology is to obtain *accurate* age constraints for extra-terrestrial samples. The critical feature of the ^{40}Ar/^{39}Ar method that allows for this is the capacity for incremental heating of samples to interrogate thermal histories. The quality of the age spectra obtained from step-heating experiments (i.e., the reproducibility of ages between sequential heating steps) will ultimately control the precision of obtained ages; this will be linked directly to sample selection and quality. Variability between steps may in fact indicate complex thermal histories that would not be identified by other means (e.g., sample in Figure 1).

The precision of ages for each incremental heating analysis is also an important factor and relies largely on the measurement precision of the ^{40}Ar/^{39}Ar ratio. Given that extra-terrestrial samples will be sufficiently old that measurable quantities of ^{40}Ar have ingrown from ^{40}K (even in low K samples), the limiting factor here will be the production of ^{39}Ar from ^{39}K by neutron irradiation. The amount of ^{39}Ar produced, along with the ability to measure small ^{39}Ar beams next to large ^{40}Ar beams (abundance sensitivity), will thus control the attainable precision of each analysis. The acceptable level of precision will likely be significantly lower than typically achieved terrestrially, which will allow for the measurement of smaller ^{39}Ar beams.

Analysis time

The time required for analysis may be a factor if this technology is implemented as one component of a larger mission. Although neutron irradiation durations will be long, the process is largely passive and thus does not require the exclusive use of mission capabilities. A multipurpose rover, for example, could be driving and/or performing other tasks during the months-long irradiation period. Sample drilling and preparation would require the use of drills and other automated sample handling components. Sample heating, particularly at higher temperature steps, would likely use much of an instrument package's power requirements, and thus during this time (typically tens of minutes), other activities would cease. Power requirements of the mass spectrometer would similarly require exclusive use of a typical power source. In terrestrial applications, gas extraction, purification and measurement are typically completed within 20–30 min per analysis. Given the need for background and discrimination measurements, as well as incremental heating of samples, each sample may require *ca.* 2 days of analytical time.

Cost

A major cost for this instrumentation involves the procurement of ^{252}Cf. Although only 43 mg is required to produce an acceptable neutron flux, this material is produced in very small quantities in only one known location. The HFIR at ORNL typically produces only *ca.* 40 mg of ^{252}Cf per year, which sells commercially at a cost of *ca.* $60000 per mg (Martin *et al.* 2000); 43 mg could thus cost $2.6 million. The cost is due to the large number of high-energy neutrons (> 2000) required to produce each atom of ^{252}Cf. The quantity required for this mission (43 mg for a source strength of 10^{11} n s^{-1} without multiplication) thus would utilise much of the available material. Further, the short $t_{1/2}$ would require that an initially higher quantity be included in the mission to account for decay during transit and that the material be made as close to launch as possible. This would require careful planning on the part of the ^{252}Cf producer (e.g., ORNL) and future mission organisers. Shipping costs do not appear to be significant at this level (Martin *et al.* 2000), but security and handling costs may also be a factor.

A second major cost involves obtaining approval to launch ^{252}Cf. Similar to the MMRTG power system on Curiosity, launch of ^{252}Cf by NASA would require an extensive environmental and safety review to show compliance with the NEPA; launches by other space programmes would require meeting policies of the particular nation. The costs involved in launch approval are difficult to estimate but could rival, or even exceed, the cost of procuring the ^{252}Cf.

The third major cost for a mission involving this technology would be costs associated with launching the instrument package. For example, recent launches to Mars have cost *ca.* $10000 per kg. Potentially high-mass components include multiplier and shield material and a high-abundance sensitivity mass spectrometer. The requirement for these materials is linked in that an improved mass spectrometer would allow for the measurement of smaller quantities of ^{39}Ar; thus, source strength could be decreased, limiting the required amounts of costly ^{252}Cf and high-mass multiplier and shielding material. Identifying the most efficient balance between these factors will play a key role in the potential for future success of the project.

Calculations towards potential solutions

Preferred solution

The preferred solution herein involves the technological development of a noble gas quadrupole or ion trap mass spectrometer for spaceflight with improved abundance sensitivity (e.g., Todd *et al.* 2007, Neidholdt *et al.* 2015). Development could focus on technologies such as those in the Hiden or Extrel instruments, which have abundance sensitivities of *ca.* 1×10^7. Technological development should in part focus on mass reduction to make the instrument more amenable to spaceflight applications.

Assuming an improved abundance sensitivity of the mass analyser to 1×10^7, it should be possible to measure with reasonable precision (5%) ^{40}Ar/^{39}Ar ratios of *ca.* 5×10^5 to obtain ^{39}Ar signals of *ca.* 50× the peak tail value. Peak tail effects can be quantitatively analysed prior to launch by measuring similarly under-irradiated samples. Calculations presented in Figure 2 indicate this is achievable by a 100-day irradiation (an arbitrary but reasonable duration) in a neutron flux of 6.73×10^8 n cm^{-2} s^{-1}. Given a source at a distance of 1 cm from the sample, this would require a source strength of 8.46×10^9 n s^{-1}, which in turn requires only 1.22 mg of ^{252}Cf (Table 1) (at a cost of *ca.* $73000). The time that will pass between ^{252}Cf manufacture and irradiation (depending on logistics and largely on flight time to destination) will require additional ^{252}Cf to account for its relatively short $t_{1/2}$ of 2.645 a.

Shielding a source, this size could be effectively accomplished with a reasonable mass of shielding material. As shown in Figure 5a, a 30 cm shield of HDPE significantly decreases the neutron energy by scattering. Data presented in Figure 8 show that *ca.* 3% of neutrons remain at the surface of a 35 cm HDPE or Premadex® shield; this flux could be further reduced by introducing a thin film of neutron-absorbing material around the neutron moderator (Figure 8b). The 35 cm HDPE shield alone would reduce the flux at the shield surface to *ca.* 6.75×10^6 n cm^{-2} s^{-1}, already under the apparent tolerance of 10^7 n cm^{-2} s^{-1} for the most sensitive components (CCD) included in the Curiosity rover mission. Assuming that shielding is only required for mission instruments (and not the planetary surface), only a small fraction of a spherical shield would be required, and this fraction would decrease with increased distance between the neutron source and other instruments. Given a 1 m distance between the source and sensitive mission components, geometry reduces the fraction of shield required to cover a 1 m high and wide instrument package to *ca.* 6% of the total sphere. Given a material density of 0.97 g cm^{-3} and the above distances, a 35 cm shield could have a mass of < 11 kg.

Further, this shield efficiency does not account for geometric effects, which reduce the flux by the inverse

square of the radius. Applied over the entire 1 m distance between the sample chamber and other instruments, this effect would act to further reduce the flux by a factor of *ca.* 0.000816 to *ca.* 5.5×10^3 n cm^{-2} s^{-1}, several orders of magnitude lower than the tolerances of the sensitive CCD components on Curiosity.

The total mass of the instrument package in this case is largely reliant on the mass of the quadrupole instrument and shielding. As noted above, shielding amounts may be limited by the use of a thinner shield, and potentially also by implementing only a partial shield to cover the other instruments. Indeed, given a similar sample chamber flux (at 1 cm from the source) of 2.25×10^8 n cm^{-2} s^{-1} and only accounting for the geometric effect, the flux at 35 cm reaches 1.8×10^5 n cm^{-2} s^{-1}. The use of distance rather than high-mass shielding material is more likely to produce an acceptably low neutron flux in an instrument package with an acceptably low mass. The quadrupole instrument mass may also be reduced through technological development and substitution of certain components for those with lower mass.

Alternative solution

An alternative approach would use existing spaceflight-ready quadrupole technology from SAM and instead focus on increasing the neutron flux. This can be accomplished by a combination of the procurement of additional ^{252}Cf and the use of ^{235}U as a neutron multiplier. Reducing the neutron flux to acceptable levels in this situation would require more shield material for two reasons: first, a higher flux requires more shielding to reach acceptable neutron flux levels for other system components, and second, this requires a larger source volume and thus larger volume of shield material to cover. For example, the abundance sensitivity of the heritage instrument on SAM is *ca.* 10^5. Reasonably precise $^{40}Ar/^{39}Ar$ ratios of *ca.* 5×10^3 should be measurable, again with signals of *ca.* 50× the peak tails. Achieving this ratio within a similar irradiation duration of 100 days requires a neutron flux of 6.73×10^{10} n cm^{-2} s^{-1}, two orders of magnitude higher than the previous case. Shielding a larger signal would subsequently require additional neutron shielding material and/or distance between the source and other neutron sensitive components.

Conclusions

The challenges and costs involved in an ambitious mission to apply $^{40}Ar/^{39}Ar$ chronology to planetary surfaces are clearly substantial – from the procurement of ^{252}Cf, to the launch of tens of kilograms of instruments, to the time requirements for analyses. However, the combination of technology described herein is feasible and has the potential to *accurately and reliably* answer a major remaining question in many extra-terrestrial environments – 'how old is it?' By selectively deploying this instrument package to any number of planetary and/or asteroidal surfaces, we can begin to decipher the history of these bodies and their places in the solar system.

We have shown that numerous related and often competing factors would be involved in the development of this technology. One potential solution, involving an improved mass spectrometer, would enhance abundance sensitivity, which perhaps provides the most feasible approach by limiting the required neutron source strength and thus required shielding. Further technological developments that improve abundance sensitivity in lower mass quadrupole instruments would allow for the extra-terrestrial application of not only $^{40}Ar/^{39}Ar$ geochronology but also other scientific functions.

Acknowledgements

We thank Roger Scott, David Gilliam and David Thomas for early discussions and suggestions in nuclear physics and ^{252}Cf. We thank Ken Farley for his continuing interest and helpful suggestions. We thank Paul Renne, Tim Becker, Karl van Bibber, Peter Hosemann, Max Fratoni, Rachel Slaybaugh, Richard Firestone and Cory Waltz for their participation in a workshop, as well as continuing discussion in geochronology, mass spectrometry, nuclear engineering and materials properties. We thank Luke Wells and Dave Seymour from Hiden Analytical and Terry Whitmore from Henniker Scientific, for discussions in quadrupole mass spectrometry. We thank UK Space Agency grant ST/M000036/1 for funding. The authors have no conflict of interest to declare. Any use of trade, product or firm names is for descriptive purposes only and does not imply endorsement by the U.S. Government. We thank three anonymous reviewers for their constructive suggestions.

References

Anderson F., Nowicki K., Hamilton V. and Whitaker T. (2012).
Portable geochronology with LDRIMS: Learning to date meteorites like Zagami with the Boulder Creek granite. Lunar and Planetary Science. Lunar and Planetary Institute (Houston, USA).

Bar-Cohen Y. and Sherrit S. (2003)
Realtime sensing while drilling using the USDC and integrated sensors. The 17th European Conference on Solid-State Transducers (Guimarães, Portugal).

references

Boehnke P. and Harrison T.M. (2016)
Illusory late heavy bombardments. Proceedings of the National Academy of Sciences United States of America, 113, 10802–10806.

Bogard D.D. and Garrison D.H. (2003)
^{39}Ar-^{40}Ar ages of eucrites and thermal history of asteroid 4 Vesta. Meteoritics and Planetary Science, 38, 669–710.

Cartwright J.A., Farley K.A., Hurowitz J.A., Asimow P.D., Simcic J., Madzunkov S. and Papanastassiou D.A. (2014)
Dating Mars with ID-KArD: Further advance for a future mission. Goldschmidt Conference (Sacramento, CA, USA), 4397.

Cassata W.S. (2014)
In situ dating on Mars: A new approach to the K-Ar method utilizing cosmogenic argon. Acta Astronautica, 94, 222–233.

Cassata W.S., Shuster D.L., Renne P.R. and Weiss B.P. (2010)
Evidence for shock heating and constraints on Martian surface temperatures revealed by ^{40}Ar/^{39}Ar thermochronometry of Martian meteorites. Geochimica et Cosmochimica Acta, 74, 6900–6920.

Cho Y., Miura Y.N. and Sugita S. (2012)
Development of a laser ablation isochron K-Ar dating instrument for landing planetary missions. International Workshop on Instrumentation for Planetary Missions (Goddard Space Flight Center, MD, USA).

Cohen B.A., Miller J.S., Li Z.-H., Swindle T.D. and French R.A. (2014a)
The Potassium-Argon Laser Experiment (KArLE): *In situ* geochronology for planetary robotic missions. Geostandards and Geoanalytical Research, 38, 421–439.

Cohen B.A., Swindle T.D. and Roark S.E. (2014b).
In situ geochronology on the Mars 2020 rover with KArLE (Potassium-Argon Laser Experiment). Lunar and Planetary Science. Lunar and Planetary Institute (Houston, USA).

United States Nuclear Regulatory Commission (2014)
NRC: 10 CFR 20.1004 Units of radiation dose.

Farley K., Hurowitz J., Asimow P.D., Jacobson N. and Cartwright J. (2013)
A double-spike method for K-Ar measurement: A technique for high precision *in situ* dating on Mars and other planetary surfaces. Geochimica et Cosmochimica Acta, 110, 1–12.

Farley K., Malespin C., Mahaffy P., Grotzinger J., Vasconcelos P., Milliken R., Malin M., Edgett K., Pavlov A. and Hurowitz J. (2014)
In situ radiometric and exposure age dating of the Martian surface. Science, 343, 1247166.

Golombek M.P., Grant J.A., Crumpler L.S., Greeley R., Arvidson R.E., Bell J.F., Weitz C.M., Sullivan R., Christensen P.R., Soderblom L.A. and Squyres S.W. (2006)
Erosion rates at the Mars Exploration Rover landing sites and long-term climate change on Mars. Journal of Geophysical Research: Planets, 111, E12S10.

Hartmann W.K. and Barlow N.G. (2006)
Nature of the Martian uplands: Effect on Martian meteorite age distribution and secondary cratering. Meteoritics and Planetary Science, 41, 1453–1467.

Hartmann W.K. and Neukum G. (2001)
Cratering chronology and the evolution of Mars. Space Science Reviews, 96, 165–194.

Hartmann W.K., Anguita J., de la Casa M.A., Berman D.C. and Ryan E.V. (2001)
Martian cratering 7: The role of impact gardening. Icarus, 149, 37–53.

Ivanov B.A. (2001)
Mars/Moon cratering rate ratio estimates. Space Science Reviews. 96, 87–104.

Jourdan F., Matzel J.P. and Renne P.R. (2007)
^{39}Ar and ^{37}Ar recoil loss during neutron irradiation of sanidine and plagioclase. Geochimica et Cosmochimica Acta, 71, 2791–2808.

Konenkov N.V., Cousins L.M., Baranov V.I. and Sudakov M.Y. (2001)
Quadrupole mass filter operation with auxiliary quadrupolar excitation: Theory and experiment. International Journal of Mass Spectrometry, 208, 17–27.

Koornneef J.M., Bouman C., Schwieters J.B. and Davies G.R. (2014)
Measurement of small ion beams by thermal ionisation mass spectrometry using new 10^{13} Ohm resistors. Analytica Chimica Acta, 819, 49–55.

Li X., Breitkreutz H., Burfeindt J., Bernhardt H.G., Trieloff M., Hopp J., Jessberger E.K., Schwarz W.H., Hofmann P. and Hiesinger H. (2011)
Evaluation of neutron sources for ISAGE – *In-situ*-NAA for a future lunar mission. Applied Radiation and Isotopes, 69, 1625–1629.

Litvak M., Mitrofanov I., Barmakov Y.N., Behar A., Bitulev A., Bobrovnitsky Y., Bogolubov E., Boynton W., Bragin S. and Churin S. (2008)
The dynamic albedo of neutrons (DAN) experiment for NASA's 2009 Mars Science Laboratory. Astrobiology, 8, 605–612.

Mahaffy P.R., Webster C.R., Cabane M., Conrad P.G., Coll P., Atreya S.K., Arvey R. and 78 others. (2012)
The sample analysis at Mars investigation and instrument suite. Space Science Reviews, 170, 401–478.

Malespin C., Mahaffy P., Farley K., Grotzinger J., Vasconcelos P., Conrad P. and Cartwright J. (2014)
Methods for *in situ* radiometric dating on Mars with Curiosity and future landers. Lunar and Planetary Science Conference, 2424.

references

Martin R.C., Knauer J.B. and Balo P.A. (2000)
Production, distribution and applications of californium-252 neutron sources. Applied Radiation and Isotopes, 53, 785–792.

McDougall I. and Harrison T.M. (1999)
Geochronology and thermochronology by the $^{40}Ar/^{39}Ar$ method. Oxford University Press (New York, USA).

McNaught A. and Wilkinson A. (1997)
International Union of Pure and Applied Chemistry (IUPAC). Blackwell Scientific Publications (Oxford, UK).

Merrihue C. and Turner G. (1966)
Potassium-argon dating by activation with fast neutrons. Journal of Geophysical Research, 71, 2852–2857.

Mitrofanov I.G., Litvak M.L., Kozyrev A.S., Mokrousov M.I., Sanin A.B. and Tretyakov V. (2005).
Dynamic Albedo of Neutrons (DAN): Active nuclear experiment onboard NASA Mars Science Laboratory. Lunar and Planetary Science. Lunar and Planetary Institute (Houston, USA).

Mitrofanov I.G., Litvak M.L., Varenikov A.B., Barmakov Y.N., Behar A., Bobrovnitsky Y.I., Bogolubov E.P., Boynton W.V., Harshman K., Kan E., Kozyrev A.S., Kuzmin R.O., Malakhov A.V., Mokrousov M.I., Ponomareva S.N., Ryzhkov V.I., Sanin A.B., Smirnov G.A., Shvetsov V.N., Timoshenko G.N., Tomilina T.M., Tret'yakov V.I. and Vostrukhin A.A. (2012)
Dynamic albedo of neutrons (DAN) experiment onboard NASA's Mars science laboratory. Space Science Reviews, 170, 559–582.

Munk M., Slaybaugh R., Van Bibber K., Morgan L.E., Davidheiser-Kroll B. and Mark D.F. (2015)
Design and feasibility study of a compact neutron source for extraterrestrial geochronology applications. Joint International Conference on Mathematics and Computation (M&C), Supercomputing in Nuclear Applications (SNA), and the Monte Carlo (MC) Method (Nashville, TN, USA).

Neidholdt E.L., Farley K., Darrach M.R., Madzunkov S.M. and Schaefer R.T. (2015)
JPL Flyby mass spectrometer. The 10th Harsh-Environment Mass Spectrometry Workshop (Baltimore, MD, USA).

Paine J.H., Nomade S. and Renne P.R. (2006)
Quantification of ^{39}Ar recoil ejection from GA1550 biotite during neutron irradiation as a function of grain dimensions. Geochimica et Cosmochimica Acta, 70, 1507–1517.

Renne P.R., Knight K.B., Nomade S., Leung K.-N. and Lou T.-P. (2005)
Application of deuteron–deuteron (D–D) fusion neutrons to $^{40}Ar/^{39}Ar$ geochronology. Applied Radiation and Isotopes, 62, 25–32.

Robbins S.J., Antonenko I., Kirchoff M.R., Chapman C.R., Fassett C.I., Herrick R.R., Singer K., Zanetti M., Lehan C., Huang D. and Gay P.L. (2014)
The variability of crater identification among expert and community crater analysts. Icarus, 234, 109–131.

Schneider B., Kuiper K., Postma O. and Wijbrans J. (2009)
$^{40}Ar/^{39}Ar$ geochronology using a quadrupole mass spectrometer. Quaternary Geochronology, 4, 508–516.

Swindle T., Bode R., Boynton W., Kring D., Williams M., Chutjian A., Darrach M., Cremers D., Wiens R. and Baldwin S. (2003).
AGE (Argon Geochronology Experiment): An instrument for in situ geochronology on the surface of Mars. Lunar and Planetary Science. Lunar and Planetary Institute (Houston, USA).

Talboys D.L., Barber S., Bridges J.C., Kelley S.P., Pullan D., Verchovsky A.B., Butcher G., Fazel A., Fraser G.W., Pillinger C.T., Sims M.R. and Wright I.P. (2009)
In situ radiometric dating on Mars: Investigation of the feasibility of K-Ar dating using flight-type mass and X-ray spectrometers. Planetary and Space Science, 57, 1237–1245.

Tanaka K.L., Skinner J.A. Jr, Dohm J.M., Irwin R.P. III, Kolb E.J., Fortezzo C.M., Latz T., Michael G.G. and Hare T.M. (2014)
Geologic map of Mars. U.S. Geological Survey Scientific Investigations Map 3292.

Taylor R. (2005)
Prometheus project final report. National Aeronautics and Space Administration, Pasadena, CA: Jet Propulsion Laboratory, National Aeronautics and Space Administration. http://hdl.handle.net/2014/38185.

Timoney R., Harkness P., Worrall K., Li X., Bolhovitins A. and Lucas M. (2015)
European ultrasonic planetary core drill. 12th International Planetary Probe Workshop (Cologne, Germany).

Todd J.F., Barber S.J., Wright I.P., Morgan G.H., Morse A.D., Sheridan S., Leese M.R., Maynard J., Evans S.T. and Pillinger C.T. (2007)
Ion trap mass spectrometry on a comet nucleus: The Ptolemy instrument and the Rosetta space mission. Journal of Mass Spectrometry, 42, 1–10.

Turner G. (1970a)
Argon-40/Argon-39 dating of lunar rock samples. Geochimica et Cosmochimica Acta Supplement, 1, 1665–1684.

Turner G. (1970b)
Argon-40/Argon-39 dating of lunar rock samples. Science, 167, 466–468.

Warner N.H., Gupta S., Calef F., Grindrod P., Boll N. and Goddard K. (2015)
Minimum effective area for high resolution crater counting of martian terrains. Icarus, 245, 198–240.